ECOLE DES MINES DE NANTES

SUBATECH

UMR Université, Ecole des Mines, IN2P3/CNRS

LABORATOIRE DE PHYSIQUE SUBATOMIQUE
ET DES TECHNOLOGIES ASSOCIEES

On the fission of ^{56}Ni and ^{48}Cr rotating nuclei

G. Royer

Rapport Interne SUBATECH - 94-14

ADRESSE ACTUELLE : **SUBATECH** - 2, RUE DE LA HOUSSINIERE. 44072 NANTES CEDEX 03. TELEPHONE 40 37 30 66 FAX 40 37 31 76
RUE MARCEL SEMBAT 44049 NANTES CEDEX 04 TELEPHONE 40 44 83 00 TELECOPIE 40 71 97 40 E-mail Farn/Bitnet @ FRCPN11 IN2P3 FR

ON THE FISSION OF ^{56}Ni AND ^{48}Cr ROTATING NUCLEI

G.ROYER

Laboratoire de Physique Subatomique et des Technologies Associées
UMR IN2P3/CNRS, Université de Nantes et Ecole des Mines de Nantes
2 rue de la Houssinière - 44072 Nantes Cedex 03 - France

Abstract : The symmetric and asymmetric fission of the ^{56}Ni and ^{48}Cr rotating nuclei has been studied within the generalized liquid-drop model including the nuclear proximity energy. The selected shape sequence allows the rapid formation of a neck while keeping spherical ends. The potential barrier is a scission barrier standing at large deformations which hinders the fission process even at very high spins. Hyperdeformed minima appear at the foot of the fission barrier for sufficiently high angular momenta. These quasi-molecular configurations might correspond to some experimentally observed resonances at high angular momenta while, for lower spins, the fission barriers are sufficiently high and wide to allow fusion-fission phenomena.

1.INTRODUCTION

Surprising resonances have been observed in the elastic and inelastic cross sections of the $^{28}Si + ^{28}Si$ (Betts et al 1981) and $^{24}Mg + ^{24}Mg$ (Zurmuhle et al 1983, Wuosmaa et al 1990) reactions. They occur at excitation energies around 60-70 MeV and angular momenta of about 35-45 $\hbar$. The properties of these resonances suggest molecule-like configurations and two-centre shell model description and coupled channel calculations (Maas and Scheid 1990, Khosla et al 1990, Uegaki and Abe 1993) have been developped. More recently, the fission of ^{56}Ni (Sanders et al 1987, 1989 and 1994, Vineyard et al 1990) and ^{48}Cr (Hasan et al 1994) has been reported. Other extensive studies of the ^{48}Cr nucleus are planed (Beck and Sanders 1994). The link between the resonance and fission processes is not yet completely understood and the discrimination between deep-inelastic orbiting and fusion-fission mechanisms is not obvious, especially at high spins. A weak absorption and the existence of pockets in the interaction potential of the two incoming ions have been advocated (Fink et al 1972) as well as the existence of shape isomeric states due to shell stabilization of highly deformed compound nuclei (Chandra and Mosel 1978, Betts et al 1981, Rae and Merchant 1992, Zhang et al 1994).

To investigate the potential energy surface within macroscopic approaches shape sequences must be selected and many parametrisations have been proposed (see the exhaustive review by Hasse and Myers 1988). The geometrical characteristics deduced from the experimental data (mainly the moment of inertia and quadrupole moment) are not sufficient to unambiguously discriminate between these shape sequences . Nevertheless, for light nuclear systems, most macroscopic approaches conclude that the compound nucleus scission and saddle shapes look like two close spherical fragments.

In the present paper, our purpose is to determine the l-dependent symmetric and asymmetric fission barriers, potential energy minima and kinetic energies of the fragments of the ^{56}Ni and ^{48}Cr nuclei. The selected shape sequence begins with the rapid formation of a neck in the nuclear matter while keeping spherical ends and leads finally to two (or three) touching spherical nuclei which go away later. The deformation energy is calculated within the generalized liquid-drop model. It includes a nuclear proximity energy term to take into account the nuclear interaction between the surfaces around the neck. This additional contribution plays a major role for such compact and very necked shapes and it has been often disregarded in the past. It allows to describe smoothly the transition from one-body to two-body shapes and flattens strongly the hill between the so-called fusion and fission valleys (Mignen et al 1988). The fission path and potential energy are described in section 2. The deformation barriers and the asymmetry and [illegible] displayed in sections 3 and 4. Finally, the kinetic energy of the fragments is given in section 5.

2.FISSION PATH AND POTENTIAL ENERGY

The selected shape sequence is displayed in figure 1. It depends only on one parameter (the ratio of the minor and major semi-axes) in the symmetric case and on two parameters when the asymmetry is taken into account (Royer and Remaud 1982 and 1985, Royer and Mignen 1992). Originally, it has been derived from inversion of oblate ellipsoids. All shape dependent functions (volume, surface, curvature, distance between the centres of mass of the nascent fragments, moment of inertia and quadrupole moment) are available analytically. This shape parametrisation allows to describe simply the continuous transition from one sphere to two (or three aligned) touching spherical fragments with the progressive formation of a deep neck. Its ability to describe the fission of light nuclei and fusion in the whole mass range is clear. For the fission of intermediate and heavy nuclei, this shape sequence is different from the most commonly admitted one but it seems that a binary fission path through this shape

sequence is not incompatible with experimental data (Royer and Remaud 1984) and might allow to explain the occurence of hyperdeformed nuclei at very high spins in the intermediate mass region (Galindo-Uribarri et al 1993, Royer and Haddad 1993). The ternary fission valley has also been investigated since hyperdeformed states having the form of a prolate $^{16}O+^{16}O+^{16}O$ molecule have been predicted within the cranked alpha cluster model (Rae and Merchant 1992) for the ^{48}Cr nucleus.

Within the generalized liquid-drop model, the deformation energy is the difference between the Coulomb, surface and proximity energies of the deformed nucleus and the ones of the initial spherical compound nucleus.

$$E_{\mathrm{def}} = \frac{3e^2Z^2}{5R_0}(B_c - 1) + a_s(1 - 2.6\,I^2)A^{2/3}(B_s - 1) + 2\gamma\int \phi(D/b)2\pi h\,dh .$$

B_c and B_s are the Coulomb and surface shape dependent functions and A, Z and I the mass, charge and relative neutron excess of the compound nucleus. The surface coefficient a_s, the effective sharp radius R_0, the surface parameter γ and the surface width b are defined as

$$a_s = 17.9439 \text{ MeV},$$
$$R_0 = 1.28A^{1/3} - 0.76 + 0.8A^{-1/3} \text{ fm},$$
$$\gamma = 0.9517(1\text{-}2.6\ I^2) \text{ MeV.fm}^{-2}$$
$$\text{and } b = 0.99 \text{ fm}.$$

R_0 equals 4.35 and 4.11 fm for ^{56}Ni and ^{48}Cr. The integration of the proximity function ϕ of Feldmeier (1979) is done in the transverse plane. h varies from the neck radius to the top of the crevice and D is the associated distance between the surfaces in regard.

While for very elongated shapes with shallow necks the contribution of the proximity energy to the deformation energy is small, its importance is decisive in the case of compact and very necked shapes. Indeed, the origin of this additional term is the strong attraction due to nuclear forces between the surfaces of the neck or the gap between the fragments and the usual surface tension energy term does not include this contribution. In this approach, the transition between the potential energy of one-body and two-body systems is smooth (this is not a trivial problem, see Swiatecki 1993) since the nuclear energy cancels naturally when the neck radius increases and the crevice disappears.

The fission and fusion barrier heights as well as fusion crosss sections which derive from this macroscopic energy have been checked in the whole mass range and the agreement is satisfactory (Royer 1986). The rotational energy $\hbar^2 l(l+1)/2I_\perp$ has been determined within the rigid body ansatz. It has been recently shown (Bencheikh et al 1993) that this approximation is reasonable since corrective terms arising from the orbital motion and the spin degrees of freedom roughly cancel each other, particularly at large deformations.

3.L-DEPENDENT DEFORMATION BARRIERS

The potential barriers encountered by the rotating ^{56}Ni and ^{48}Cr nuclei during their deformation and eventual fission or, in the entrance channel, the fusion barriers standing in front of the $^{28}Si + ^{28}Si$, $^{32}S + ^{24}Mg$, $^{40}Ca + ^{16}O$, $^{24}Mg + ^{24}Mg$, $^{20}Ne + ^{28}Si$ and $^{36}Ar + ^{12}C$ systems are displayed in figures 2 and 3. The saddle point (top of the barrier) corresponds always to two separated nuclei maintained in unstable equilibrium by the balance between the repulsive Coulomb forces and the attractive nuclear proximity forces. Precisely, for the ^{56}Ni and ^{48}Cr nuclei respectively, the distances at the saddle point between the sharp equivalent surfaces of the two equal fragments are 2.2 and 2.3 fm while the distances between the centres of mass are 9.1 and 8.9 fm ; the proximity energy reaching still - 2.4 and - 1.9 MeV. For the six above mentioned reactions, the fusion barrier heights are respectively 28.6, 28.0, 23.6, 21.5,

21.0, and 16.4 MeV. With these values the fusion cross sections for the $^{28}Si + ^{28}Si$ and $^{40}Ca + ^{16}O$ reactions have been accurately reproduced (Royer and Remaud 1983 and Royer 1986).

If one looks at the exit channel, with increasing angular momenta the compound nucleus moves from the spherical shape to hyperdeformed configurations corresponding to two quasi-spherical fragments connected by a small bridge of matter. The fragment separation occurs before reaching the maximum of the potential barrier which is consequently a scission barrier standing at large deformations. The moment of inertia and the curvature are high at the barrier top and the potential pocket can only be removed by the centrifugal forces for high angular momenta of about 40-45 $\hbar$. In such a deformation path, there is no more distinction between pockets in the interaction potential of the two incoming ions and external shape isomeric minima in the fission barrier of the compound nucleus.

The link between these macroscopic calculations and the informations concerning high-spin resonance-like structure and fusion-fission reactions is still rather speculative and further experimental data are needed. Nevertheless, resonances at excitation energies of 60 to 70 MeV and spin from 36 to 42 $\hbar$ have been observed in $^{28}Si + ^{28}Si$ reaction (Betts et al 1981) while, in $^{24}Mg + ^{24}Mg$ scattering, tentative spins of 36, 38 and 40 $\hbar$ have been assigned to three resonant states at saddle-point energies from 63 to 70 MeV (Zurmuhle et al 1983, Wuosmaa et al 1990). Our calculated excitation energy and spin range agrees roughly with these experimental data. The resonances might correspond to unstable and non equilibrated nuclear systems evolving on the quasi-plateau of the potential barriers for the highest spins. In contrast, the fusion-fission events would be connected with fusing systems which would have attained the hyperdeformed minima at lower spins. These systems would be more equilibrated since the high external scission barrier hinders the fission process and allows the mixture of the nuclear matter.

Ternary fission barriers for ^{48}Cr are displayed in figure 4. Let us recall that Rae and Merchant (1992) calculated that the hyperdeformed states having the form of a $^{16}O+^{16}O+^{16}O$ molecule are stable up to high spins of 60 $\hbar$ corresponding to very high excitation energies of about 120 MeV above the bandheads. In our approach and in the symmetric ternary fission path, hyperdeformed minima corresponding to three aligned quasi-spheres connected by deep necks exist also for spins from 23 to 60 $\hbar$ and excitation energies from 35 to 105 MeV. Shell effects are not included in our calculations and the predicted hyperdeformed states are only due to the influence of the macroscopic rotational energy, the choice of the shape sequence which allows to push the potential barrier towards large deformations and the introduction of the proximity energy. For low spins, shell stabilization can introduce prolate or oblate deformations around the sphere but for larger deformations the slope of the potential energy curve is very pronounced and it seems little likely than superdeformed states due to shell effects may survive.

The fission barriers and the maximal angular momentum than the nuclei can sustain are much lower in the binary fission valley than in the ternary one. Nevertheless, it is quite striking to observe that the deformation energy of the minimum in the 25-40 $\hbar$ range is of the same order or lower in the symmetric ternary decay channel than in the binary one and that its position is more external (higher moment of inertia). Then, it seems that one may not exclude the occurence of prolate $^{16}O+^{16}O+^{16}O$ molecular configurations following fusion reactions in this spin and excitation energy range.

4.ASYMMETRY AND SPIN DEPENDENCE OF THE POTENTIAL BARRIERS

The moments of inertia of the hyperdeformed minima, the saddle-point energies and the fission barrier heights are plotted as functions of the angular momentum and the mass asymmetry in figures 5, 6 and 7. The moment of inertia increases with the symmetry of the

reaction since the matter distribution of the quasi-molecular shapes is farther from the rotation axis. It increases also with the spin since the potential pocket is progressively pushed at the foot of the external scission barrier. Experimentally, more data are needed to precisely assign a moment of inertia to the observed structures.

At low spins, the saddle-point energies decrease with the mass-asymmetry coordinate, this was expected since these light nuclei are located below the Businaro-Gallone point where the symmetric saddle-point loses its stability. On the contrary, at high spins, the saddle-point energies raise strongly with the asymmetry allowing to attain very high excitation energies (difference between the saddle-point energy and the fission barrier height) of about 80-90 MeV. Correlated with the saddle-point energies, the fission barrier heights decrease with the mass asymmetry at low spins while for the highest angular momenta they tend to increase for very high asymmetry. Such a behavior is different from the one deduced from the approach of Sierk (1986) within the study of the binary decay of ^{56}Ni formed in the ^{32}S + ^{24}Mg reaction (Sanders et al 1989, figure 11). They obtain progressively, with increasing spins, an independence of the saddle-point energies on the mass asymmetry, the maximal excitation energy being about 60 MeV for a critical angular momentum of 45 $\hbar$. Therefore It would be interesting to further investigate (in the exit as well as in the entrance channel) very asymmetric reactions at very high excitation energies to see whether such resonances still exist.

5.KINETIC ENERGY OF THE FRAGMENTS

The total kinetic energy of the fragments is the potential energy at the scission point plus the possible pre-scission kinetic energy. In our approach the point where the rupture of the bridge of matter between the nascent fragments occurs is not the scission point since it is located before reaching the top of the barrier. The scission point corresponds to the position where the proximity forces end to act. It is more external and lower than the saddle-point on the potential barrier. As an example, assuming that $|E_{prox}| < 0.1$ MeV, the distance between the surfaces of the fragments is 4.4 fm for ^{56}Ni. The TKE is then only the Coulomb repulsion energy at this point. It is displayed in figure 8 for ^{56}Ni and ^{48}Cr. For the symmetric fission of ^{56}Ni formed in the ^{32}S + ^{24}Mg reaction at E_{cm} = 60.5 MeV the experimental value is 38.0 ± 1.5 MeV. Sanders et al (1989) obtain 38.4 MeV for l = 36 $\hbar$. For this spin value, our calculations give E_{cm} = 59.8 MeV and E_k = 38.1 MeV. The agreement is quite satisfactory.

6.CONCLUSION

The symmetric and asymmetric fission of ^{56}Ni and ^{48}Cr rotating nuclei has been studied within the generalized liquid-drop model including the nuclear proximity energy. The selected shape sequence describes the continuous transition from one sphere to two (or three aligned) tangent spherical fragments which go away later. The l-dependent potential barrier stands at large deformations. The top corresponds to two separated spheres still under the influence of the attractive nuclear forces. Hyperdeformed minima appear at the foot of the fission barrier for sufficiently high angular momenta. Some experimentally observed resonances at high spins might be connected with these quasi-molecular configurations while, for lower angular momenta, fusion-fission phenomena can occur since the scission barrier is sufficiently high and wide to allow the mixture of the nuclear matter before the fission. The existence of ^{16}O+^{16}O+^{16}O molecular states seems also possible at intermediate spins.

Further experiments are strongly desirable to better know the spin, the moment of inertia, the maximal excitation energy and the dependence on the asymmetry of these strongly deformed states in ^{56}Ni and ^{48}Cr nuclei.

FIGURE CAPTIONS

Figure 1 : Shape sequence leading rapidly to quasi-molecular binary and ternary configurations. Volume conservation is assumed.

Figure 2 : Sum of the macroscopic deformation and rotational energies as functions of the moment of inertia and angular momentum ($\hbar$ unit) for $^{28}Si + ^{28}Si$, $^{32}S + ^{24}Mg$ and $^{40}Ca + ^{16}O$ systems. The vertical dashed and dotted curve indicates the position of the two spherical nuclei in contact.

Figure 3 : L-dependent deformation barriers versus the moment of inertia and spin ($\hbar$ unit) for $^{24}Mg + ^{24}Mg$, $^{20}Ne + ^{28}Si$ and $^{36}Ar + ^{12}C$ systems. The position of the two spherical nuclei in contact is given by the vertical dashed and dotted curve.

Figure 4 : Ternary fission barriers for ^{48}Cr leading to the systems : $^{16}O + ^{16}O + ^{16}O$ and $^{20}Ne + ^{8}Be + ^{20}Ne$.

Figure 5 : Rigid moment of inertia ($\hbar^2 . MeV^{-1}$ unit) of the strongly deformed potential energy minima versus the angular momentum ($\hbar$ unit) and the mass asymmetry.

Figure 6 : Saddle-point energies as functions of mass asymmetry and spin for the ^{56}Ni and ^{48}Cr compound nuclei.

Figure 7 : Fission barrier heights as functions of mass asymmetry and spin for the ^{56}Ni and ^{48}Cr compound nuclei.

Figure 8 : Kinetic energy of the two fragments as functions of asymmetry and angular momentum for the ^{56}Ni and ^{48}Cr compound nuclei.

REFERENCES

Beck C and Sanders SJ 1994 private communications
Bencheikh K, Quentin P, Bartel J and Meyer J 1993 Nucl.Phys.A**557** 459c
Betts RR, Back BB and Glagola BG 1981 Phys.Rev.Lett **47** 23
Chandra H and Mosel U 1978 Nucl.Phys.A**298** 151
Feldmeier H 1979 12th Summer School on Nucl.Physics, Mikolajki, Poland
Fink HJ, Scheid W and Greiner W 1972 Nucl.Phys.A**188** 259
Galindo-Uribarri A et al 1993 Phys.Rev.Lett **71** 231
Hasan AT et al 1994 Phys.Rev.C**49** 1031
Hasse RW and Myers WD 1988 Geometrical relationships of macroscopic nuclear physics (Berlin : Springer)
Khosla HS, Malik SS and Gupta RK 1990 Nucl.Phys.A**513** 115
Maas R and Scheid W 1990 J.Phys.G : Nucl.Part.Phys.**16** 1359
Mignen J, Royer G and Sebille F 1988 Nucl.Phys.A**489** 461
Rae WDM and Merchant AC 1992 Phys.Lett B**279** 207
Royer G 1986 J.Phys.G : Nucl.Phys.**12** 623
Royer G and Haddad F 1993 Phys.Rev.C**47** 1302
Royer G and Mignen J 1992 J.Phys.G : Nucl.part.Phys **18** 1781
Royer G and Remaud B 1982 J.Phys.G : Nucl.Phys.**8** L159
Royer G and Remaud B 1983 J.Phys.G : Nucl.Phys.**9** 1103
Royer G and Remaud B 1984 J.Phys.G : Nucl.Phys.**10** 1057
Royer G and Remaud B 1985 Nucl.Phys.A**444** 477
Sanders SJ et al 1987 Phys.Rev.Lett.**59** 2856
Sanders SJ, Kovar DG, Back BB, Beck C, Henderson DJ, Janssens RVF, Wang TF and Wilkins BD 1989 Phys.Rev.C**40** 2091
Sanders SJ et al 1994 Phys.Rev.C**49** 1016
Sierk AJ 1986 Phys.Rev.C**33** 2039
Swiatecki WJ 1993 Lawrence Berkeley Laboratory report LBL 34928 to be published
Uegaki E and Abe Y 1993 Prog.Th.Phys.**90** 615
Vineyard MF et al 1990 Phys.Rev.C**41** 1005
Wuosmaa AH, Zurmuhle RW, Kutt PH, Pate SF, Saini S, Halbert ML and Hensley DC 1990 Phys.Rev.C**41** 2666
Zhang J, Merchant AC and Rae WDM 1994 Phys.Rev.C**49** 562
Zurmuhle RW, Kutt PH, Betts RR, Saini S, Haas F and Hansen O 1983 Phys.Lett.B**129** 384

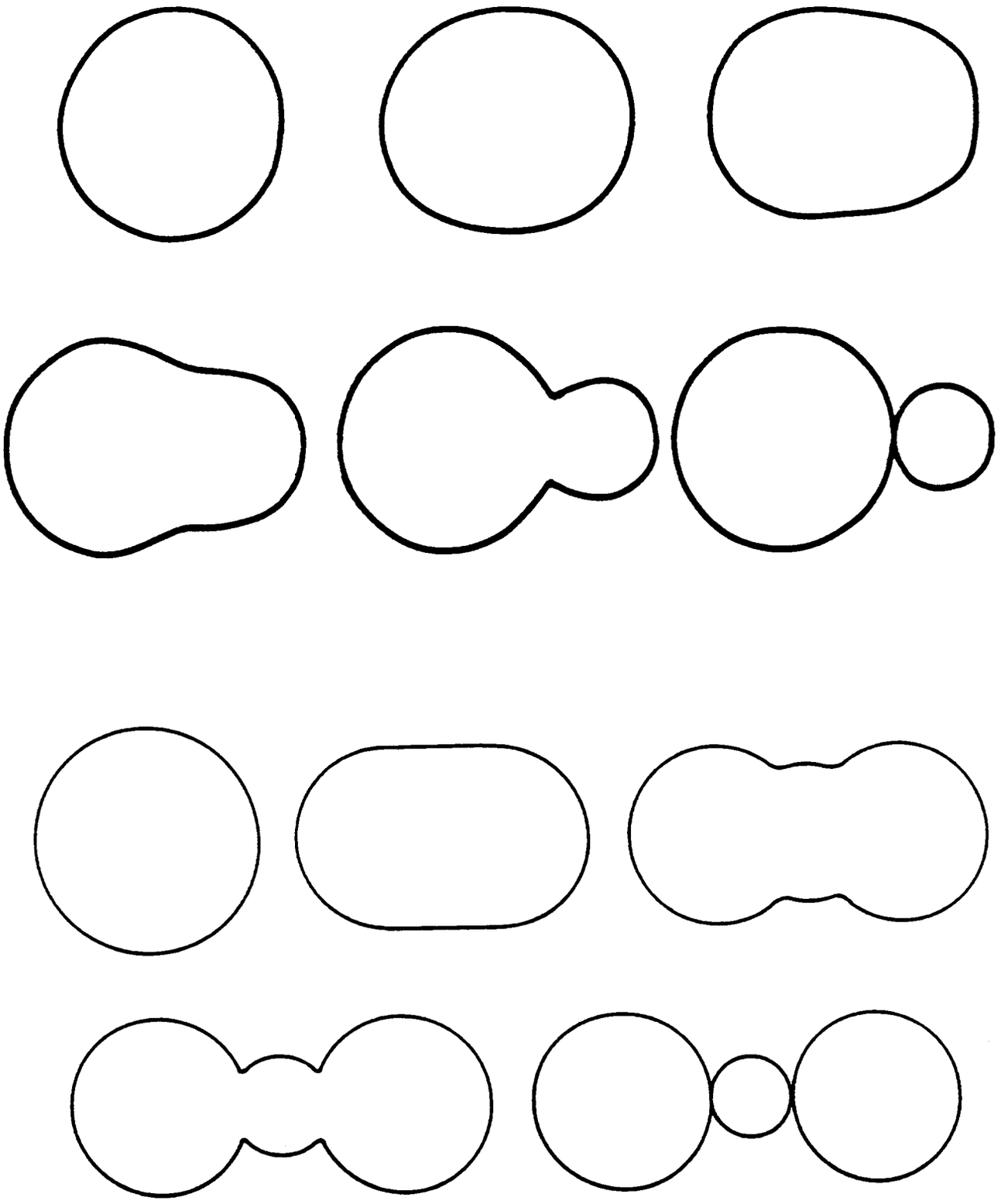

Figure 1

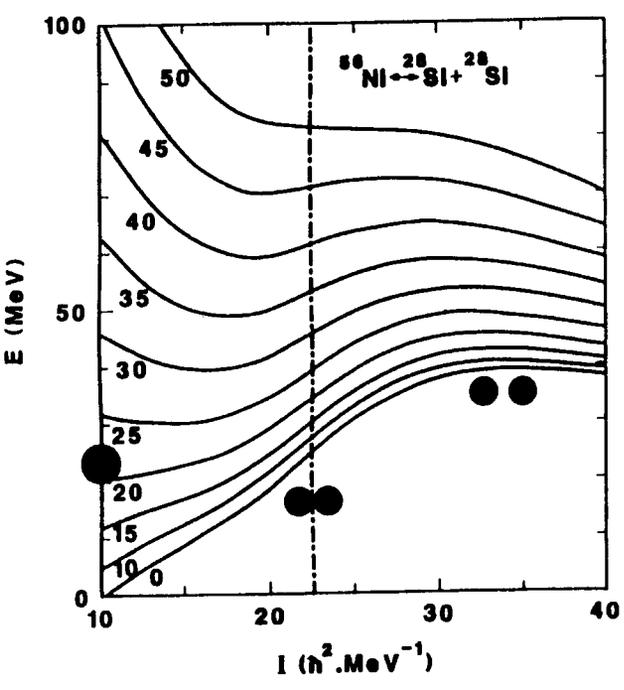

Figure 2a

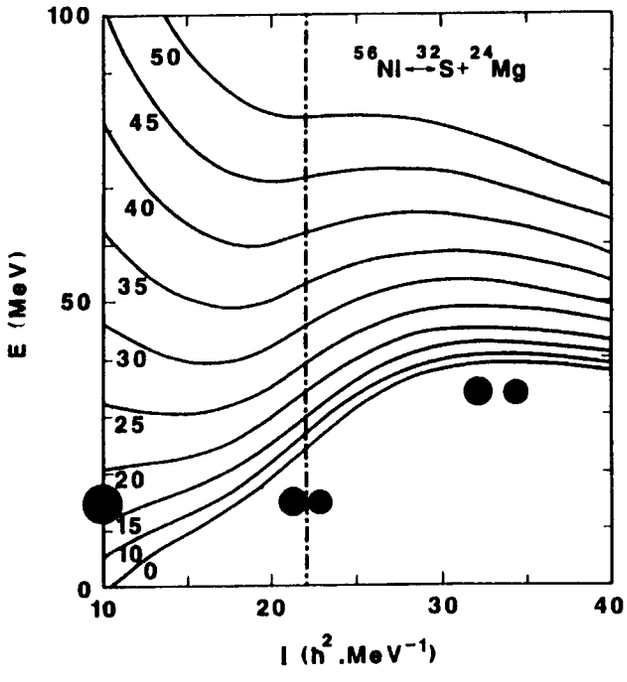

Figure 2b

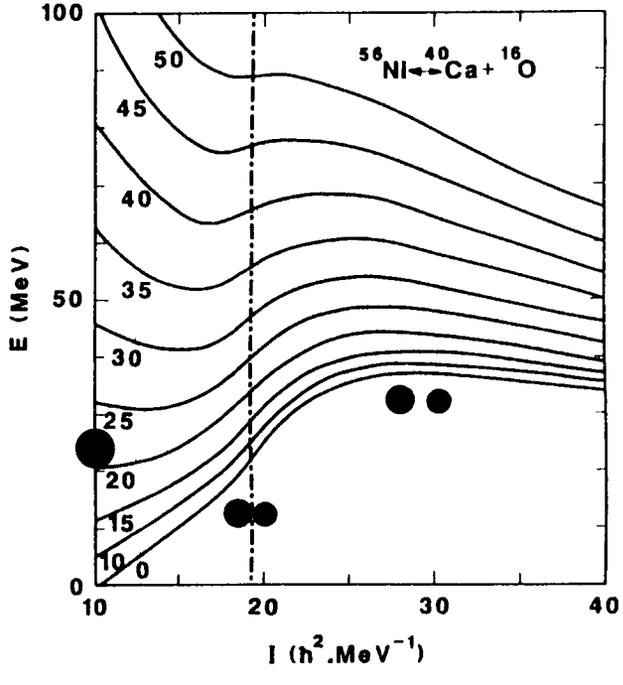

Figure 2c

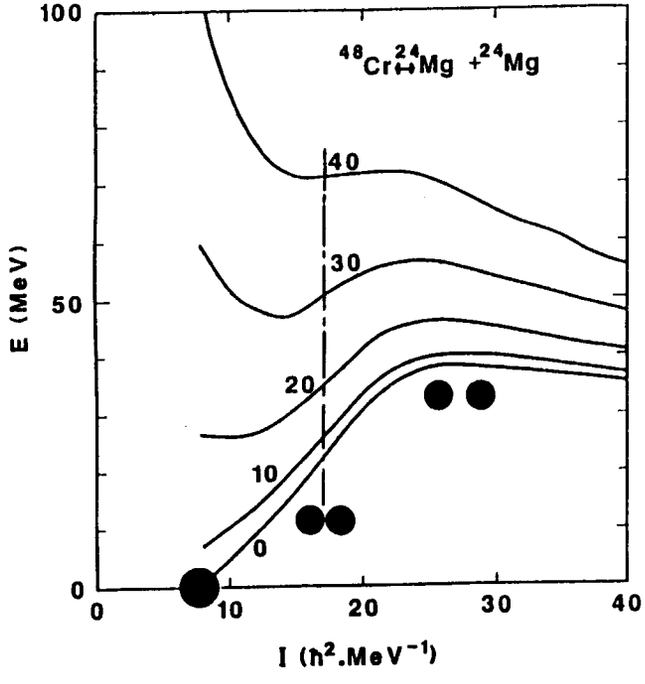

Figure 3a

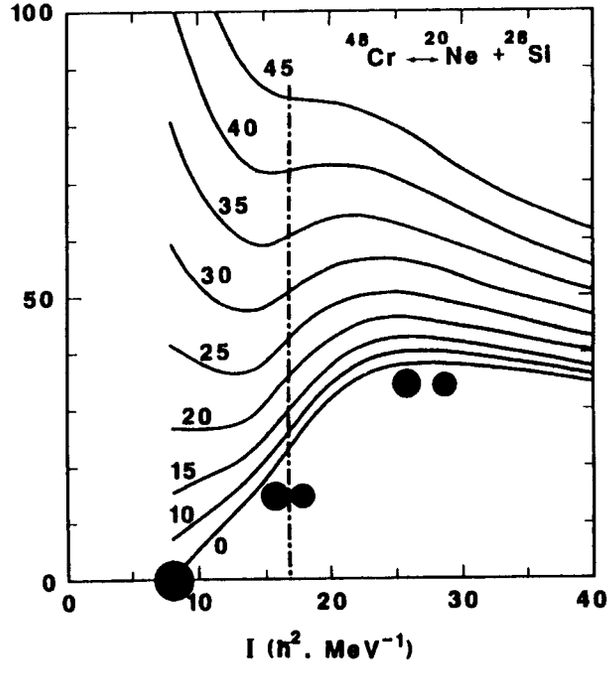

Figure 3b

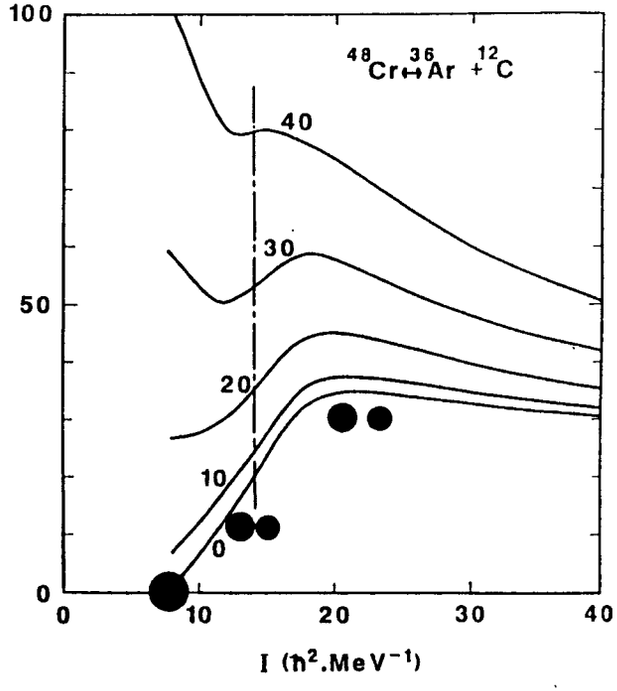

Figure 3c

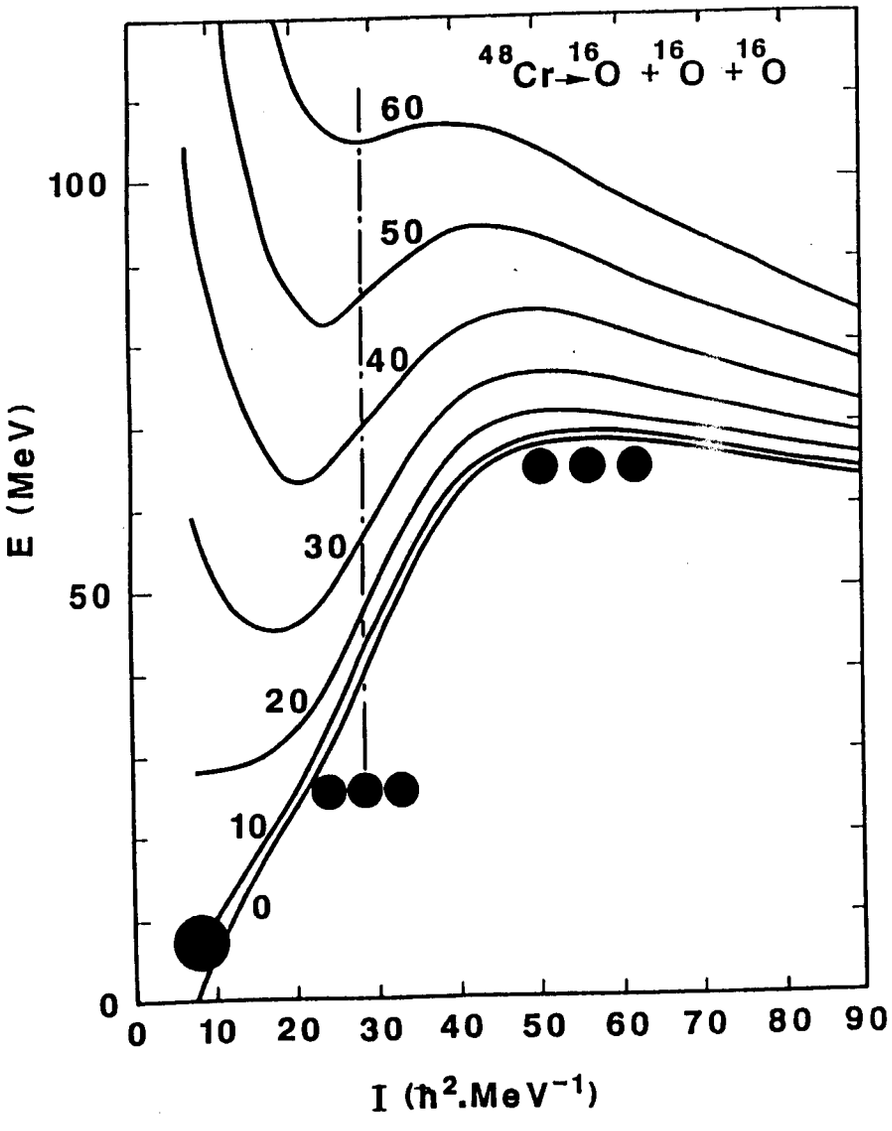

Figure 4a

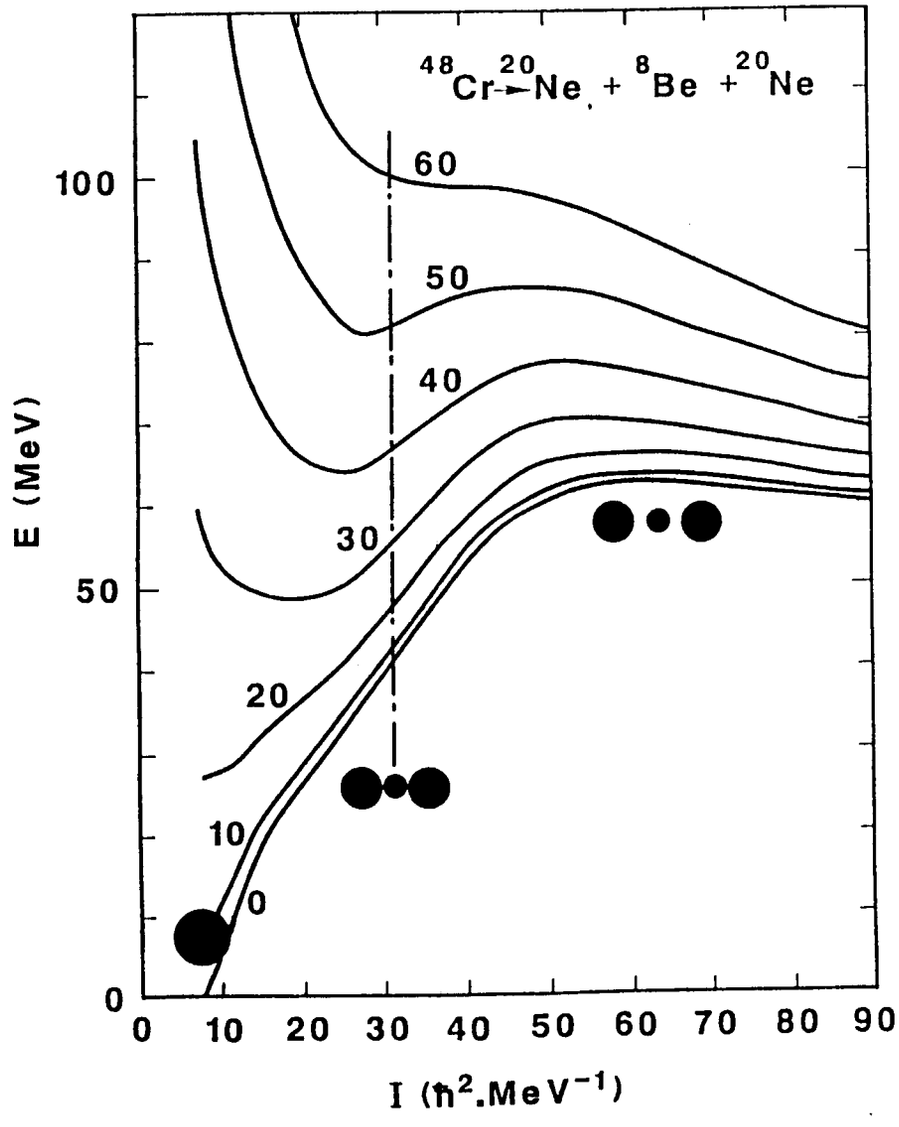

Figure 4b

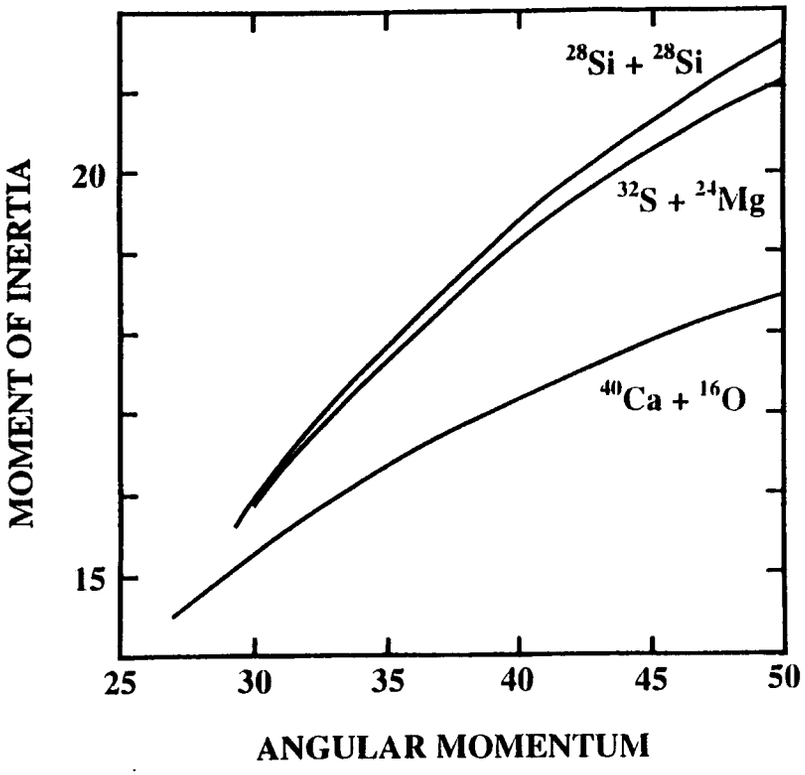

Figure 5a

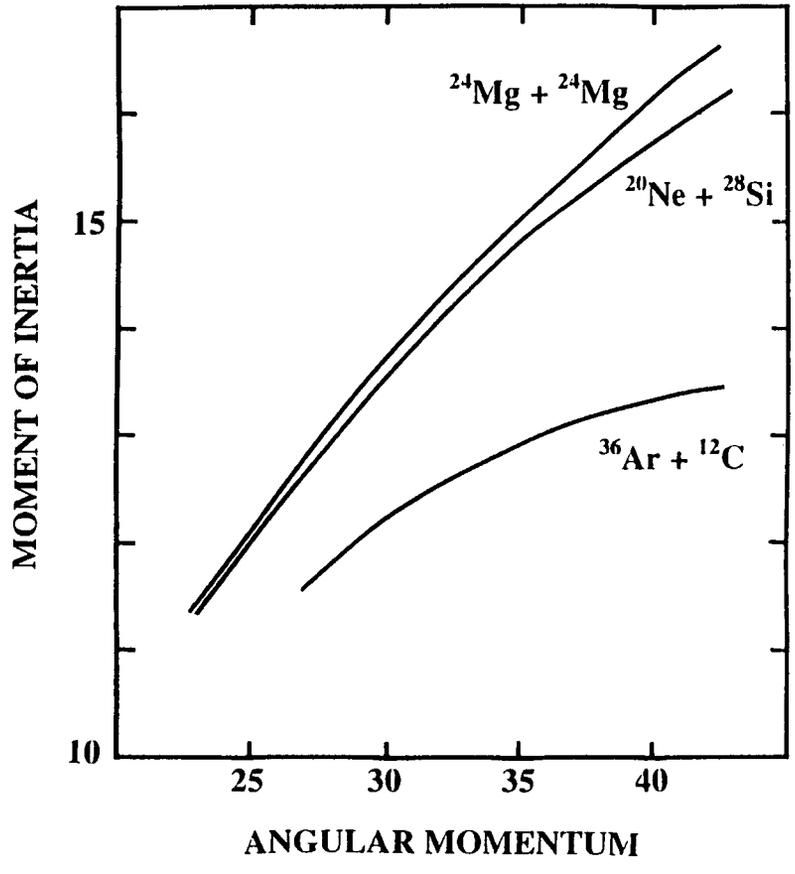

Figure 5b

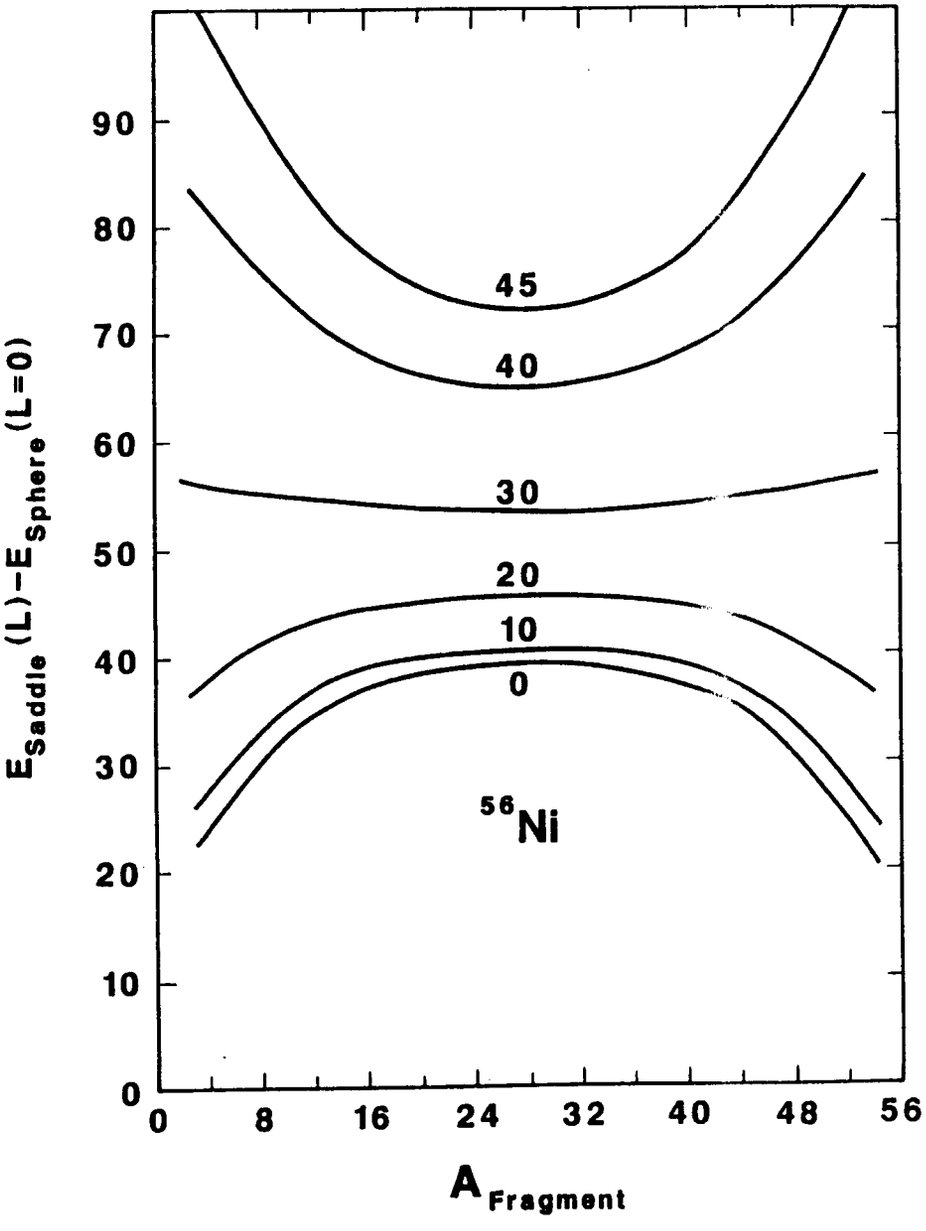

Figure 6a

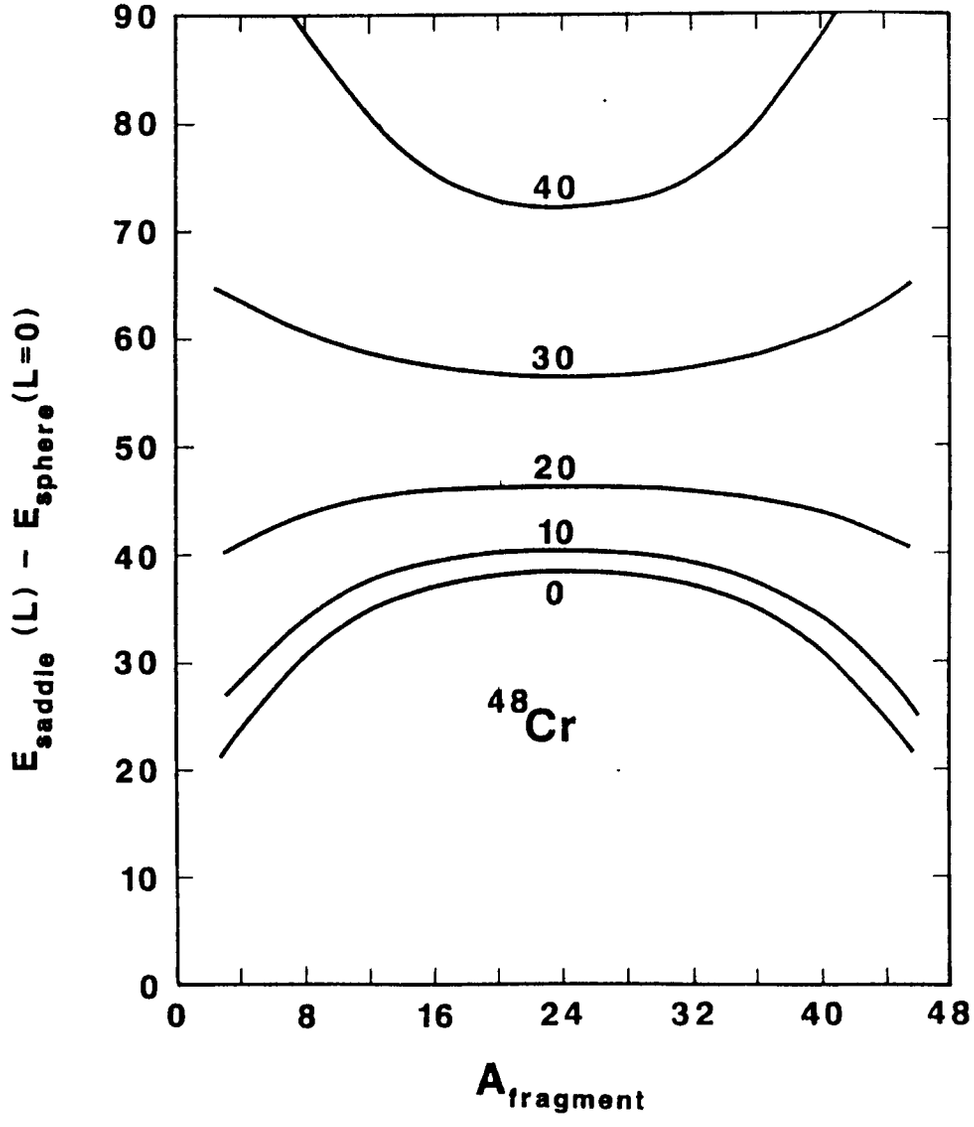

Figure 6b

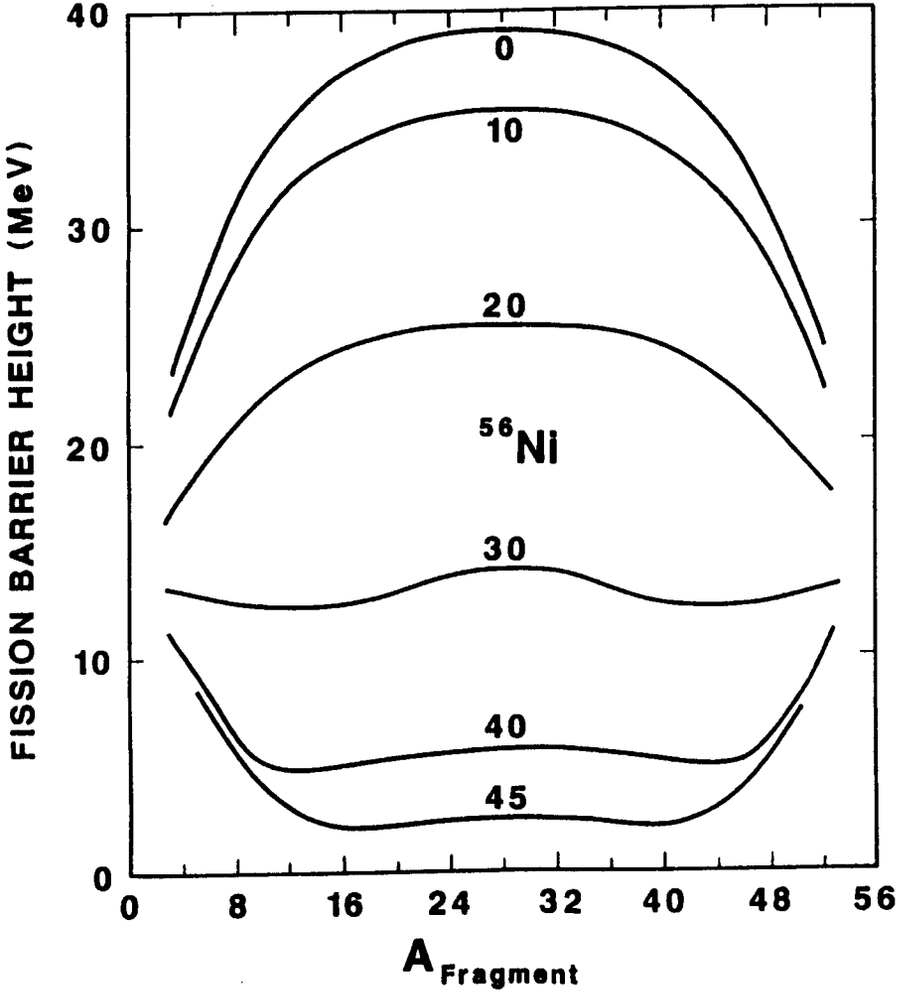

Figure 7a

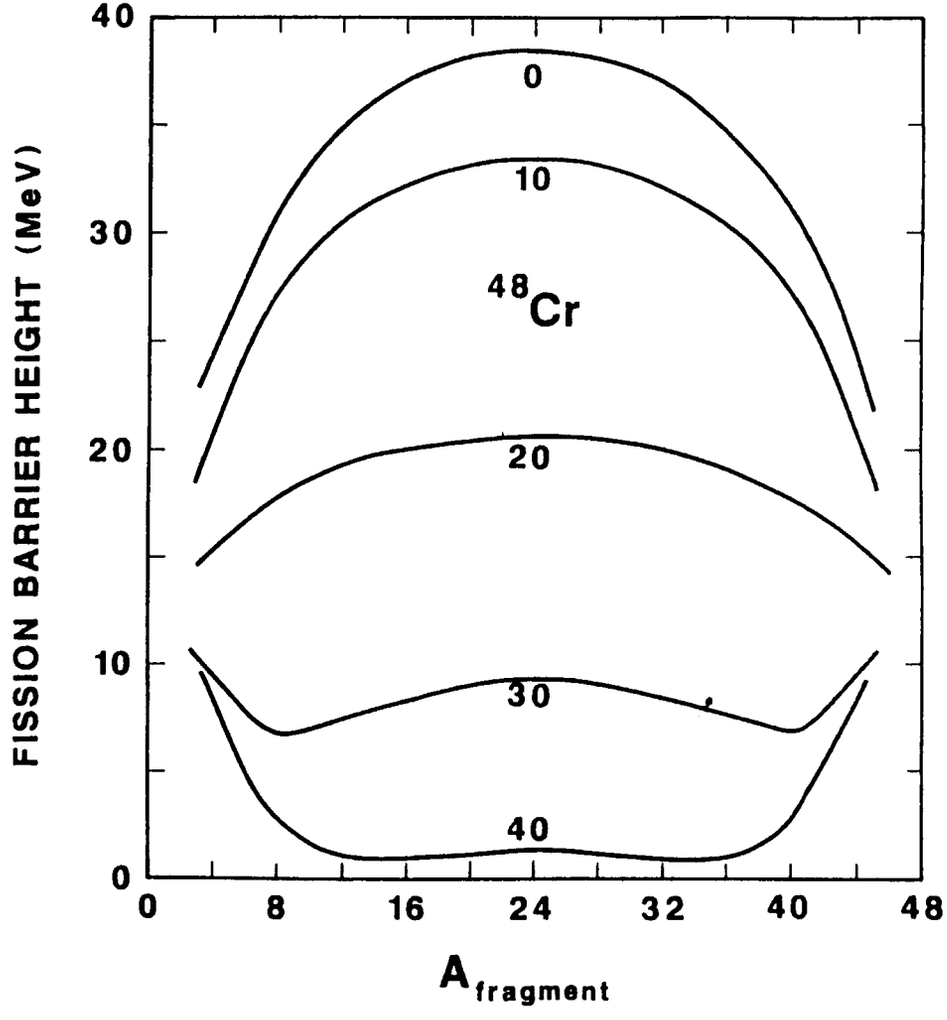

Figure 7b

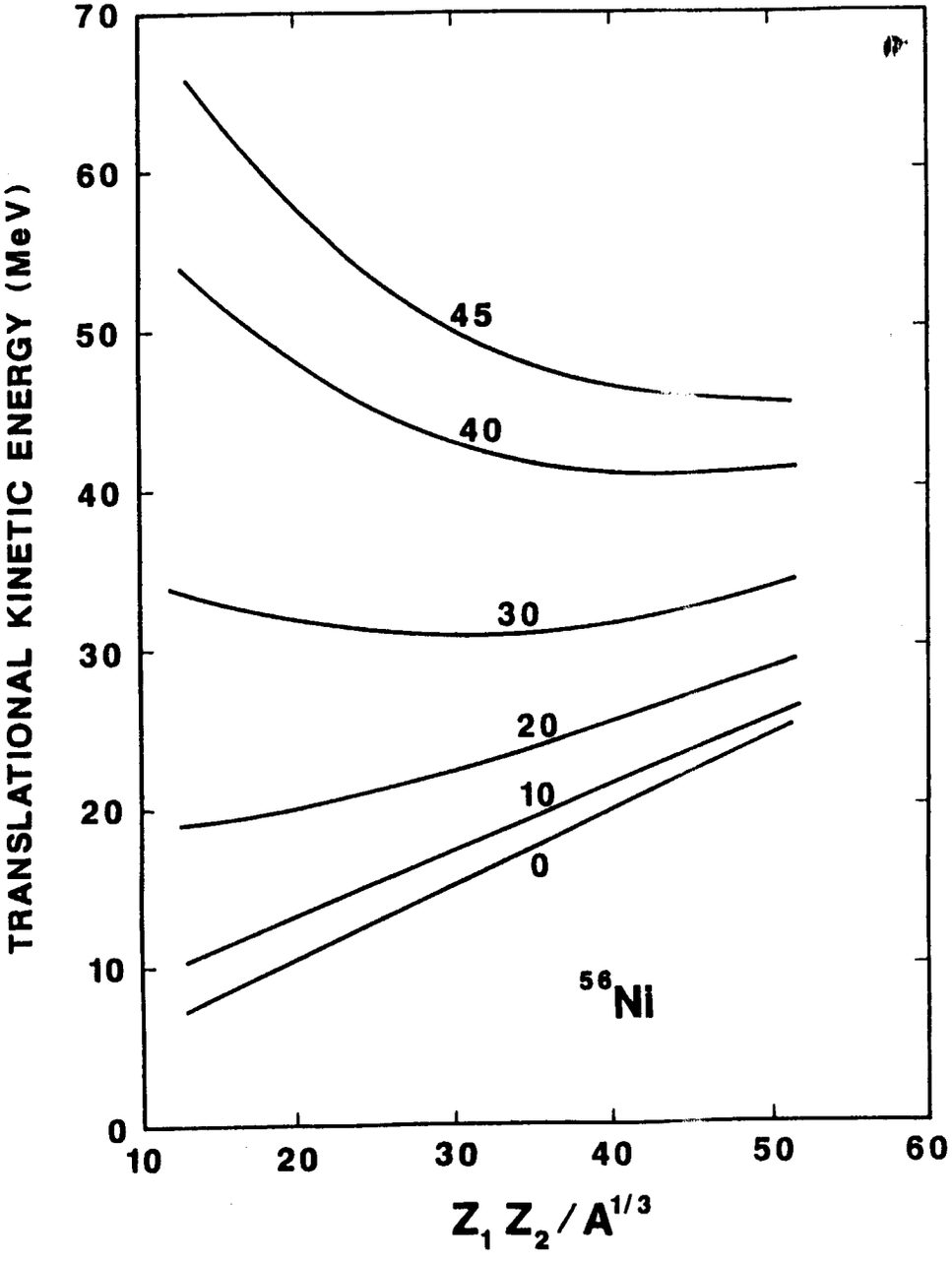

Figure 8a

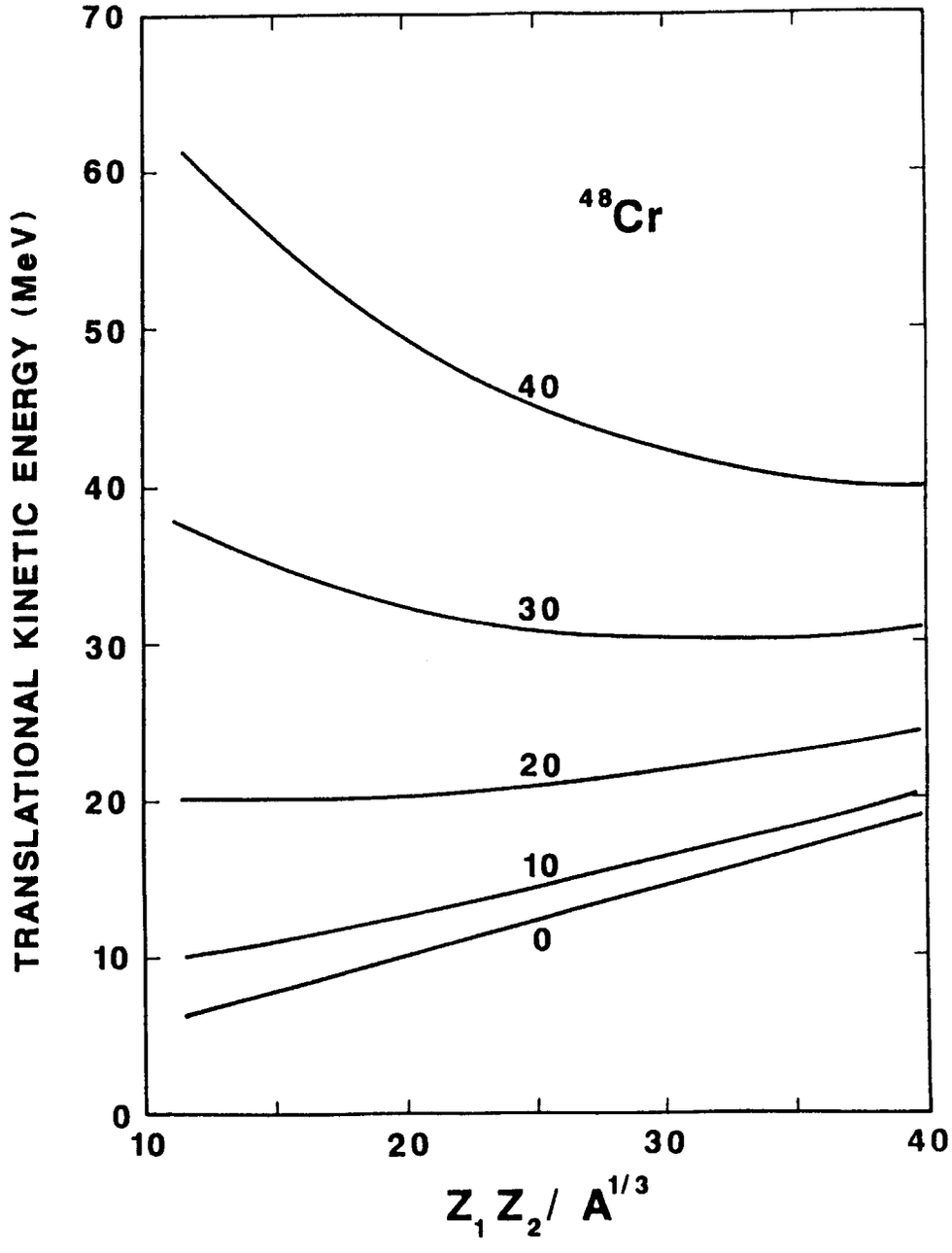

Figure 8b